Effect of electron-hole inhomogeneity on specular Andreev reflection and Andreev retroreflection in a graphene-superconductor hybrid system

Shu-guang Cheng, Hui Zhang, and Qing-feng Sun

Phys. Rev. B **83**, 235403 — Published 3 June 2011

DOI: 10.1103/PhysRevB.83.235403

Effect of electron-hole inhomogeneity on specular Andreev reflection and Andreev retroreflection in a graphene-superconductor hybrid system

Shu-guang Cheng,[1,2] Hui Zhang,[3] and Qing-feng Sun[3,*]
[1] *Department of Physics, Northwest University, Xi'an 710069, China*
[2] *National photoelectric technology and Functional Materials and Application of Science and Technology International Cooperation Base*
[3] *Institute of Physics, Chinese Academy of Sciences, Beijing 100190, China*

The electron-hole inhomogeneity in graphene has been confirmed to be a new type of charge disorder by recent experiments, and the largest energy displacement of electron and hole puddles with respect to the Dirac point can reach nearly $30meV$. Here we focus on how electron-hole inhomogeneity affects the specular Andreev reflection as well as Andreev retroreflection. In a four-terminal graphene-superconductor hybrid system, we find that the Andreev coefficients can hardly be affected even under rather large electron-hole inhomogeneity (typically $30meV$), and the boundary distinguishing two Andreev reflections can well hold, although the charge puddles strength $W = 30meV$ is much larger than the superconductor gap $\Delta = 1meV$. Furthermore when charge puddles are two orders larger than superconductor gap, a specific kind of Andreev reflection can be still obviously detected. In order to quantitatively describe what degree of the boundary blurred, a quantity D is introduced which measures the width of a crossover region between specular Andreev reflection and retroreflection in energy space. We confirm that the boundary blurring are much smaller than the charge puddles strength W. In addition, we study the effect of Anderson disorder as well for comparison, and find that the boundary is held much more obviously in this case. Finally, the fluctuations of Andreev reflection coefficient are studied. Under a typical experimental charge puddles, the fluctuations are very small when energy of the particles is away from the boundary, again confirming that the retroreflection and specular reflection can be clearly distinguished and detected in the presence of electron-hole inhomogeneity.

PACS numbers: 74.45.+c, 73.23.-b

I. INTRODUCTION

Graphene,[2–5] a new and ideal two-dimensional material with peculiar electronic properties, has attracted many attentions in the past few years since it was successfully fabricated in 2004.[6–8] At low energy, the graphene has the linear dispersion relation $E = \pm\hbar\nu_F|\mathbf{k}|$ with the Fermi velocity ν_F and its carriers are described by massless Dirac relativistic equation,[3,9] leading to many peculiar phenomena, such as relativistic Klein tunneling[10] and Veselago lensing in a graphene p-n junction[11] *etc.* Besides, the transport properties of graphene are also unique, and recently they have been broadly studied in various mesoscopic devices: like the graphene based p-n junction,[12,13] spin valve,[14] Aharonov-Bohm ring[15] and graphene-superconductor hybrid systems.[2,16–19] For example, in a graphene based Josephson junction, which is realized by coupling two superconducting electrodes to a graphene layer in experiments,[18] a nonzero supercurrent occurs even at zero carrier concentration while the Fermi level is located at the Dirac point.[16]

The transport property at the graphene-superconductor interface is of great interest as well. Specifically, the characteristic of specular Andreev reflection proposed by Beenakker in 2006.[2,19] Regular Andreev reflection occurs at the interface between a normal metal and superconductor, in which an incident electron from the metal is retroreflected as a hole while a Cooper pair forms in the superconductor.[20] Situation changes when the Andreev reflection occurs at the interface between graphene and superconductor, since the direction of reflected hole can be along the specular direction. In detail, the usual Andreev retroreflection occurs only when electron-hole conversion is of intra-band, i.e. both incident electron and reflected hole are from conduction band or valence band. On the other hand, if the electron-hole conversion is interband (i.e., the incident electron and reflected hole are respectively in conduction and valence bands), the specular Andreev reflection occurs. From standpoint of the incident electron energy E and the Dirac-point energy E_0, while $|E| < |E_0|$, both incident electron and reflected hole will be in the same band and it is the Andreev retroreflected. On the other hand, while $|E| > |E_0|$, the incident electron and reflected hole are in different bands so that it is the specular Andreev reflection. Thus $|E| = |E_0|$ is the boundary of the retroreflected and specular reflection. After the work by Beenakker, a great deal sequent works have investigated the Andreev reflection in the graphene-superconductor device.[21,22] Several methods have been proposed for the confirmation of the existence of specular Andreev reflection.[21,22]

In the two-terminal graphene-superconductor device, both Andreev retroreflection and specular Andreev reflection usually exist. Recently, we have suggested to manipulate and separate the retroreflection and specular reflection in a four-terminal graphene-superconductor hybrid system, which has two superconductor terminals.[22]

A specific type of Andreev reflection can be obtained by adjusting the superconductor phase difference θ. When the phase difference $\theta = 0$, the specular reflection disappears because of the destructive quantum interference and only the retroreflection occurs. On the other hand, while $\theta = \pi$, the retroreflection vanishes and the specular reflection exists only. Therefore, a clear boundary emerges at $|E| = |E_0|$. On the one side of $|E| = |E_0|$, the Andreev reflection coefficient is zero, but on the other side it has finite values.

In the experiment, the disorder always exists more or less. Due to the disorder, the on-site energies of carbon atoms can have a random departure from the Dirac point, which induces magnificent variation of density of states and correspondence different characters of transport properties.[23,24] For example, the disorder in a graphene p-n junction can result in some extra conductance plateaus,[12,13] and the existence of charge puddle disorder may be responsible for the minimum conductance.[25] Recently, the experiment[26] has confirmed that the charge puddle disorder (the electron-hole inhomogeneity) indeed exists. In particular, the strength of the electron-hole puddle can approximately reach $30meV$ and the size of such puddle is about several nanometers.[27,28] In a clean graphene sample Dirac point is well defined at which local density of states vanishes, while it is not in the presence of disorder. Now Dirac point has the energy fluctuation with the same strength as the disorder. In this situation the Andreev retroreflection and specular Andreev reflection seem to be chaotic due to the not well-defined Dirac points. Since a typical superconductor energy gap is about $1meV$ which is much less than the energy fluctuation $30meV$ of Dirac point, one question naturally arises: could it still be possible to distinguish the two kinds of Andreev reflections? Is the boundary $|E| = |E_0|$ of the retroreflection and specular reflection still clear? These questions are not limited only in the four-terminal graphene-superconductor interference system. For the general graphene-superconductor hybrid system, the questions still keep. Intuitively, the blurring of the boundary should be in the same order of the energy fluctuation of the Dirac point, accordingly the two kinds of Andreev reflections can not be distinguished clearly any more while the strength of disorder is $30meV$.

In this paper, we theoretically investigate the effect of the disorder on the boundary distinguishing Andreev retroreflection and specular Andreev reflection. We consider a four-terminal graphene-superconductor hybrid system consisting of two superconductor leads coupled to a zigzag edged graphene ribbon, as shown in Fig.1(a). The two superconductor leads have a phase difference θ and there exists disorder in the center region of graphene. Here two kinds of disorders, the Anderson disorder and electron-hole inhomogeneity (charge puddle disorder), are considered. By using the non-equilibrium Green's function method, the Andreev reflection coefficients can be calculated. We find that, the Andreev coefficients can hardly be affected under rather large electron-hole

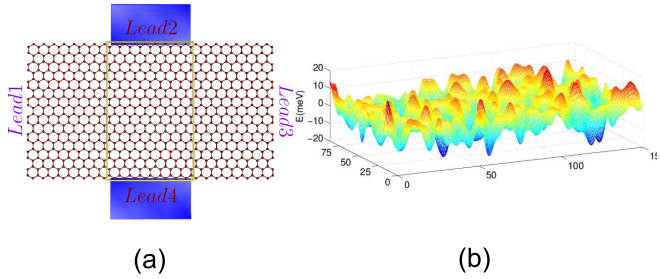

FIG. 1: (Color online) (a): Schematic diagram of a four terminal graphene-superconductor hybrid system. Leads 1 and 3 are zigzag edged graphene terminals while leads 2 and 4 are superconductor terminals. The electron-hole inhomogeneity is assumed to occur only in the center region with the size $N \times N$ illustrated as the middle rectangular area where $N = 8$. (b): Illustration of spatial charge inhomogeneity in graphene with $W = 30meV$, where red parts (packets) and blue parts (dips) are electron puddles and hole puddles respectively.

inhomogeneity (typically $30meV$ as in experiment), and the boundary at $|E| = |E_0|$ of the retroreflection and specular reflection is very clear, so two kinds of Andreev reflections can be also well distinguished. Even if in the case of very large puddle disorder (e.g., two orders larger than the superconductor gap), a specific kind of Andreev reflection can be still obviously detected, and the boundary at $|E| = |E_0|$ still exists. In order to quantitatively describe to what degree the boundary is blurred, a quantity D of boundary blurring is introduced. The D-W relation under different puddles correlation parameter and superconductor gap is studied as well. In general, when strength of electron-hole inhomogeneity W is $20meV$, the boundary blurring D is about $0.05meV$ and $D/W \approx 0.003$ only. In addition, we study the effect of Anderson disorder for comparison, and found that the boundary at $|E| = |E_0|$ is held much more obviously in this case, and $D/W \approx 0.0003$. Finally, the fluctuations of Andreev reflection coefficients are studied. Except for in the vicinity of the boundary $|E| = |E_0|$, the fluctuation almost has very small value for a typical disorder strength $W = 30meV$, again confirming that, the disorders have little effect on Andreev reflections as well as the boundary lying at $|E| = |E_0|$, accordingly the retroreflection and specular reflection can be clearly distinguished.

The rest of this paper is organized as follows. In section II, we give the tight-binding Hamiltonian of graphene-superconductor hybrid system with electron-hole inhomogeneity, the Keldysh non-equilibrium Green's function method for calculating Andreev reflection coefficients, and correspondence parameters. Numerical results and detailed discussions are demonstrated in section III. Finally, we summarize our results in Section IV.

II. MODEL AND HAMILTONIAN

We consider a four-terminal system consisting of a zigzag edged graphene ribbon symmetrically coupled by two superconductor leads as seen in Fig.1(a). The graphene ribbon with width N is divided into three parts: the terminal 1, center region, and the terminal 3. The electron-hole inhomogeneity is assumed to occur only in the center region. The terminals 2 and 4 are superconductor leads.

In the tight-binding representation, the Hamiltonian of the graphene ribbon is given by:

$$H_G = \sum_{i\sigma}(E_0+\varepsilon_i)a^\dagger_{i\sigma}a_{i\sigma} - t\sum_{<ij>,\sigma} a^\dagger_{i\sigma}a_{j\sigma} \tag{1}$$

where t denotes the nearest neighbor hopping energy, $a^\dagger_{i\sigma}$ ($a_{i\sigma}$) is the creation (annihilation) operator of electron with spin $\sigma \in \{\uparrow,\downarrow\}$ at the ith site. Being the on-site energy of carbon atoms, E_0 stands for the energy of Dirac points. Finally, the electron-hole inhomogeneity in the center region is represented by ε_i (see Fig. 1(b)), with the value given by[29]

$$\varepsilon_i = \frac{\sum_j \tilde{\varepsilon}_j \exp\left(-|\mathbf{r}_{ij}|^2/2\eta^2\right)}{\sqrt{\sum_j \exp\left(-|\mathbf{r}_{ij}|^2/\eta^2\right)}} \tag{2}$$

where η is the spatial correlation parameter and $|\mathbf{r}_{ij}|$ is the distance between site i and j. The sum of j runs over all sites in the center region. Here $\tilde{\varepsilon}_j$ is the uncorrelated on-site energy in the center region subjecting to a Gaussian distribution with zero mean and a variance W.[30] In the case of Anderson disorder, ε_i in the center region is set by a uniform random distribution within $[-W/2, W/2]$ with W being the disorder strength.

We use BCS Hamiltonian to describe superconductor leads,[31]

$$\begin{aligned} H_{S\alpha} = &\sum_{\mathbf{k}\sigma}\varepsilon_k C^\dagger_{\mathbf{k}\sigma,\alpha}C_{\mathbf{k}\sigma,\alpha} \\ &+\sum_{\mathbf{k}}(\Delta_\alpha C_{\mathbf{k}\downarrow,\alpha}C_{-\mathbf{k}\uparrow,\alpha} + \Delta^*_\alpha C^\dagger_{-\mathbf{k}\uparrow,\alpha}C^\dagger_{\mathbf{k}\downarrow,\alpha}) \end{aligned} \tag{3}$$

where $\alpha = 2, 4$ is the index of the superconductor leads, and $\Delta_\alpha = \Delta e^{i\theta_\alpha}$ is the superconductor order parameter with gap Δ and phase θ_α. In Eq.(3), we have set the chemical potential of the superconductor leads being zero as the energy zero point. The coupling between superconductor leads and graphene is described by[22,31]

$$H_{T\alpha} = \sum_{i\sigma} t a^\dagger_{i\sigma}C_{\alpha,\sigma}(x_i) + H.c. \tag{4}$$

in which x_i denotes the horizonal position of the ith carbon atom, and $C_{\alpha,\sigma}(x) = \sum_{k_x,k_y} e^{ik_x x}C_{\mathbf{k}\alpha,\sigma}$.[22,31] Here the chemical potential of superconductor leads ε_k is set to be the zero energy level. Thus the whole Hamiltonian of graphene-superconductor hybrid system is described by

$$H = H_G + \sum_{\alpha=2,4}(H_{S\alpha} + H_{T\alpha}) \tag{5}$$

By using the non-equilibrium Green's function method, the Andreev reflection coefficients T_{11A} and T_{13A} for the incident electron coming from the terminal 1 with energy E and the hole reflected to terminals 1 and 3 can be obtained:[22,31]

$$\begin{cases} T_{11A}(E) = \mathrm{Tr}\{\mathbf{\Gamma}_{1\uparrow\uparrow}\mathbf{G}^r_{\uparrow\downarrow}\mathbf{\Gamma}_{1\downarrow\downarrow}\mathbf{G}^a_{\downarrow\uparrow}\}, \\ T_{13A}(E) = \mathrm{Tr}\{\mathbf{\Gamma}_{1\uparrow\uparrow}\mathbf{G}^r_{\uparrow\downarrow}\mathbf{\Gamma}_{3\downarrow\downarrow}\mathbf{G}^a_{\downarrow\uparrow}\}. \end{cases} \tag{6}$$

where the subscripts $\uparrow\uparrow$, $\uparrow\downarrow$, $\downarrow\uparrow$, and $\downarrow\downarrow$ represent the 11, 12, 21, and 22 matrix elements respectively in the Nambu representation. The retarded and advanced Green functions in Nambu representation are defined by $\mathbf{G}^r(E) = [\mathbf{G}^a(E)]^\dagger = (E\mathbf{I} - \mathbf{H_c} - \sum_{\alpha=\mathbf{1},\mathbf{2},\mathbf{3},\mathbf{4}}\mathbf{\Sigma}^\mathbf{r}_\alpha)^{-1}$. Here $\mathbf{H}_c$ is the Hamiltonian of the center region labeled by a rectangular area as seen in Fig.1(a), and $\mathbf{I}$ is the identity matrix with the same dimension as $\mathbf{H}_c$. The coupling between center region and lead α is accounted by the retarded self-energy $\mathbf{\Sigma}^r_\alpha(E) = tg^r_{\alpha,ij}(E)t$, where $g^r_{\alpha,ij}(E)$ is the surface Green's function of lead α. In Eq. (6), the linewidth function $\mathbf{\Gamma}_\alpha(E)$ is defined with the aid of self-energy as $\mathbf{\Gamma}_\alpha(E) = i[\mathbf{\Sigma}^r_\alpha - (\mathbf{\Sigma}^r_\alpha)^\dagger]$.

The surface Green's function of the graphene terminals (i.e., leads 1 and 3) can be obtained through a standard numerical calculation procedure.[32] For the superconductor terminals (leads 2 and 4), the surface Green's function is obtained analytically,[31,33]

$$\mathbf{g}^r_{\alpha,ij}(E) = -i\pi\rho\beta(E)J_0[k_F(x_i-x_j)]\begin{pmatrix} 1 & \Delta_\alpha/E \\ \Delta^*_\alpha/E & 1 \end{pmatrix}, \tag{7}$$

where ρ is the normal density of states, $J_0[k_F(x_i-x_j)]$ is the 0th order Bessel function with the Fermi wave vector k_F, and $\beta(E) = -iE/\sqrt{\Delta^2-E^2}$ for $|E| < \Delta$ and $\beta(E) = |E|/\sqrt{E^2-\Delta^2}$ for $|E| > \Delta$. In the following numerical simulations, we set the Fermi wave-vector $k_F = 1\mathring{A}^{-1}$ and the superconductor gap $\Delta = 1meV$ (except in Fig.3(b)) as energy unit, which is approximately $t/2750$ with t being the hopping energy ($t \simeq 2.75eV$). The spatial correlation parameter of electron-hole inhomogeneity is set as $\eta = 3.5nm$ (except in Fig. 3(a)) so that the size of charge puddle is approximately $3nm \times 3nm$.[27] The size of the center region is depicted by $N \times N$ with N describing the size of the graphene ribbon. Specifically, the width of ribbon is $(3N-1)a$ and the length of the center region is $\sqrt{3}Na$ with $a = 0.142nm$ being the length of C-C bond in graphene. Hereafter, we set N as $N = 50$. In this size the center region has dozens of charge puddles. A typical charge inhomogeneity for the parameters $W = 30meV$, $\eta = 3.5nm$ and $N = 50$ is shown in Fig.1(b). Finally, while in the presence of disorder, the Andreev reflection coefficients and their fluctuations are averaged over up to 1000 random configurations.

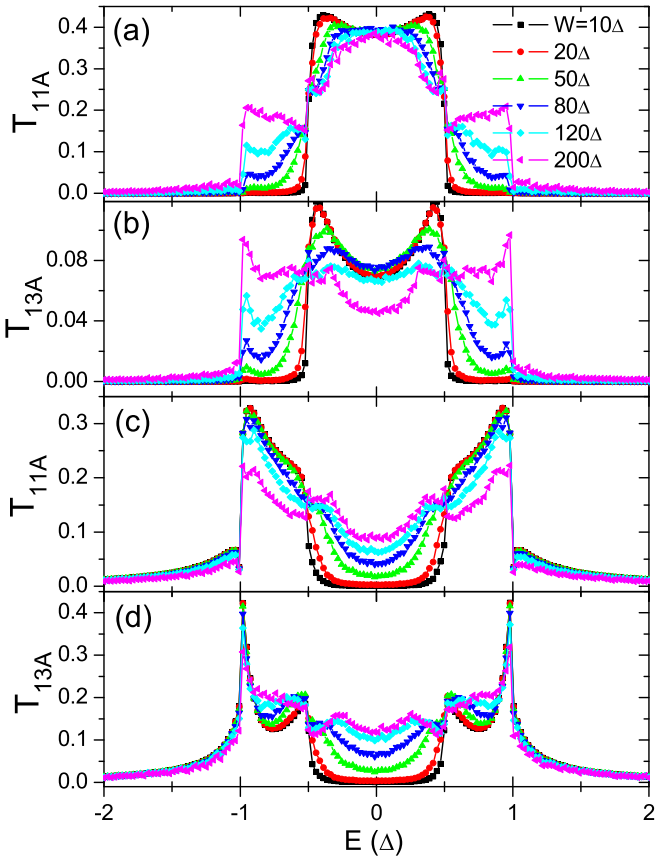

FIG. 2: (Color online) Andreev reflection coefficients T_{11A} and T_{13A} versus energy E with superconductor phase difference $\theta = 0$ (in panel (a) and (b)) and $\theta = \pi$ (in panel (c) and (d)), where the different curves are for different strengths W of charge inhomogeneity. Other parameters unmentioned are $N = 50$, $\eta = 3.5nm$ and $E_0 = -0.5\Delta$.

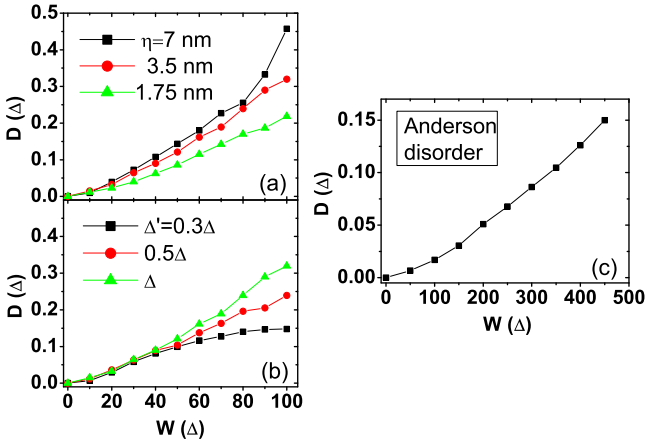

FIG. 3: The net discrepancy D in the case of $\theta = 0$ versus the disorder strength W is shown in two cases: charge puddles disorder (a and b) and Anderson disorder (c). The parameters are: in panel (a) $N = 50$ and $\Delta = 1meV$ with different η values and in (b) $N = 50$ and $\eta = 3.5nm$ with different superconductor gap (here we let Δ' be the superconductor gap and the sign $\Delta = 1meV$ still keeps). The data in the charge puddles case (for $\Delta = 1meV$, $N = 50$ and $\eta = 3.5nm$) are extracted from Fig.2(a) and in the Anderson disorder case, the data are from Fig.4(a) .

III. NUMERICAL RESULTS AND DISCUSSION

While in the absence of disorders for the four-terminal graphene-superconductor hybrid system, the Andreev retroreflection and specular Andreev reflection can be manipulated and separated by adjusting the superconductor phase difference θ.[22] Specifically, the Andreev retroreflection disappears at $\theta = \pi$, while the specular reflection vanishes at $\theta = 0$. A clear boundary emerges at $|E| = |E_0|$. On the one side of boundary, the Andreev reflection coefficients T_{11A} and T_{13A} are all zeros, whereas they have large values on the other side. In detail, while $\theta = 0$, T_{11A} and T_{13A} are zeros on the side of $|E| > |E_0|$, whereas while $\theta = \pi$, they are zeros on the side of $|E| < |E_0|$. Hereafter, we focus on the effect of the disorder on the boundary $|E| = |E_0|$ and investigate whether the two kinds of Andreev reflections can be distinguished while in the presence of disorder. In Fig.2, we show the Andreev reflection coefficients T_{11A} and T_{13A} under different electron-hole inhomogeneity disorder strength W with the phase difference $\theta = 0$ and $\theta = \pi$. We can see that, for small disorder strength W (e.g., $W = 10\Delta$), T_{11A} and T_{13A} are almost the same as that under $W = 0$. Andreev reflections occur only on the side of $|E| < |E_0|$ when $\theta = 0$, while situation reverses at $\theta = \pi$, resulting that a boundary clearly distinguishing two kinds of Andreev reflections lies exactly at $|E| = |E_0|$ regardless of $\theta = 0$ or π. With increasing the disorder strength W (e.g., $W = 20\Delta, 50\Delta$), by intuition Andreev retroreflection and specular Andreev reflection seem to become chaotic since W at the moment has been ten times larger than superconductor gap Δ and Andreev reflections occur mainly within the gap ($|E| < |\Delta|$).[34] Conversely, from Fig.2, the boundary at $|E| = |E_0|$ is found to remain clear even the disorder strength reaches 80Δ. That's to say, the blurring of boundary of retroreflection and specular reflection is much smaller than disorder strength W, and a certain kind of Andreev reflection can be still detected with charge puddles. Of course, if the disorder strength W is very large (e.g. $W = 200\Delta$), Andreev reflections become totally chaotic and the boundary disappears. In the experiment, a typical disorder strength W is about $20meV$ (20Δ), and the largest displacement of electron (hole) puddles with respect to Dirac points is reported $\approx 30\Delta$.[26,28] Under these experimental disorder strengthes, the boundary can clearly hold and two kinds of Andreev reflections can be perfectly distinguished.

Next, in order to quantitatively describe to what degree the boundary at $|E| = |E_0|$ is blurred by the disorder, we introduce a quantity D of boundary blurring which is defined as the discrepancy due to the disorder. Specifically, D value can be extracted from Fig.2(a) as

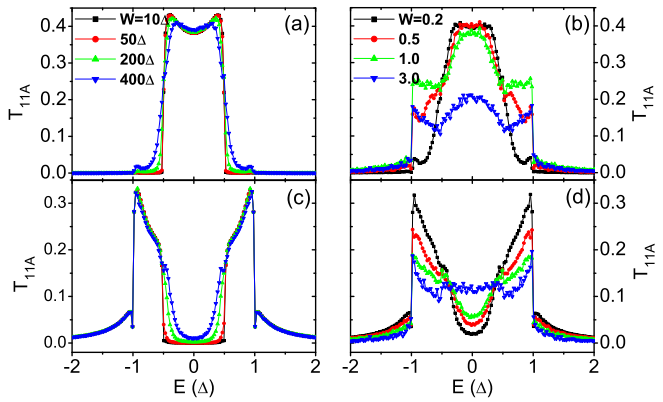

FIG. 4: (Color online) Andreev retroreflection coefficients T_{11A} versus energy E under different Anderson disorder strengths W in two cases: $\theta = 0$ (in panel (a) and (b)) and $\theta = \pi$ (in panel (c) and (d)), where W varies from 10Δ to 400Δ in (a) and (c), while from $0.2t$ to $3.0t$ in (b) and (d). The parameters unmentioned are the same as in Fig.2.

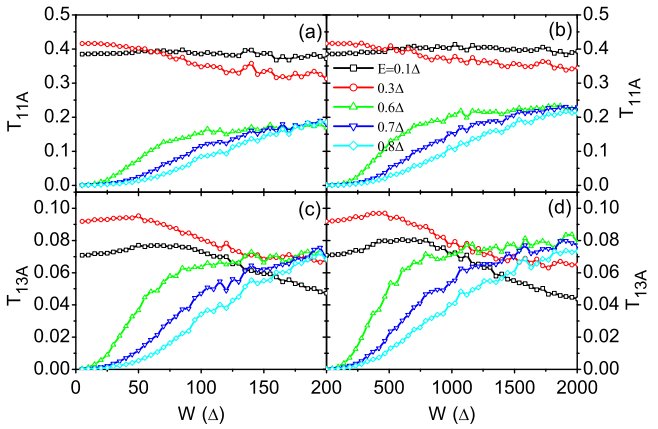

FIG. 5: (Color online) T_{11A} and T_{13A} versus disorder strength W are shown in both charge puddle disorder (in panel (a) and (c)) and Anderson disorder (in panel (b) and (d)) at $\theta = 0$, where the different curves are for different energies E. The parameters unmentioned are the same as in Fig.2.

follows. Under any specific disorder strength W, the curve T_{11A} has crossing points with the horizontal lines 0.1 and 0.3, and we denote the abscissas of the crossing points as E_1 and E_2 respectively ($E_1 > 0, E_2 > 0$). Accordingly we have $\widetilde{D}(W) \equiv |E_2 - E_1|$, and then D is defined as $D(W) \equiv \widetilde{D}(W) - \widetilde{D}(0)$. Because that the Andreev reflection coefficient T_{11A} rapidly varies in the vicinity of the boundary $|E| = |E_0|$, the net discrepancy D can well describe the degree of blurred boundary due to disorder. Fig.3(a) and (b) show D as a function of disorder strength of electron-hole inhomogeneity W under different spatial correlation length η and the superconductor gap. From Fig.3(a) and (b), we find that D always monotonously but very slowly increases with the increase of W, indicating that the boundary at $|E| = |E_0|$ becomes to blur in the presence of charge disorder, but it is not obvious. Specifically, for a typical experimental electron-hole puddle disorder strength ($W \approx 20\Delta$), D is less than 0.06Δ in all cases and $D/W \approx 0.003$. For a very large disorder strength (e.g. $W = 100\Delta$), D is still less than 0.5Δ in all cases in Fig.3(a) and (b). In other words, the boundary blurring is much smaller than the disorder strength W.

Let us study the origination of the small ratio D/W. In the presence of the disorder, the on-site energy $E_0 + \epsilon_i$ is a Gaussian distribution with the fluctuation (or variance) W. Let us introduce the mean on-site energy $\bar{E}_0$, and it is defined as $\bar{E}_0 \equiv \sum_{i=1}^{N_s}(E_0 + \epsilon_i)/N_s$ where N_s is the total site number in the center region. Due to the disorder, the mean on-site energy $\bar{E}_0$ (in other words, the mean Dirac point energy) for a specific disorder configuration usually is not equal to E_0 and so it has the fluctuation. However, the fluctuation of $\bar{E}_0$ is much smaller than W, and it can approximatively be W/N_p with N_p being the electron and hole puddle number in the center region. From the above numerical results, D is near the fluctuation of $\bar{E}_0$. This means that the boundary blurring D is mainly determined by the fluctuation of the mean value of on-site energies over the whole center region.

Furthermore, let us discuss the effect of the systemic parameters (spatial correlation parameter η and the superconductor gap) on D in detail. We find that with η increasing, D is increased for any given impurity strength W (see Fig.3a). From Eq.(2), we can see that the smaller η value corresponds to weaker correlation of on-site energies, and then there are more electron-hole puddles in the center region, leading that the smaller fluctuation of $\bar{E}_0$ and the smaller ratio D/W are. In the limit of $\eta \to 0$, the on-site energies is totally uncorrelated and the charge puddles model becomes similar to Anderson disorder model. So D/W of the Anderson disorder always is smaller than the charge puddle disorder (see below). Besides, Fig.3(b) shows D is almost independent on the superconductor gap while $W < 50\Delta$, because that the D/W is mainly determined by the fluctuation of $\bar{E}_0$. On the other side, while $W > 50\Delta$ D is slightly larger for the larger superconductor gap.

So far we have investigated the effect of charge puddle disorder on the boundary of two kinds of Andreev reflections. Besides, there is another significant kind of charge disorder, named Anderson disorder, which has been investigated broadly in the past few years.[13,35] In the following we investigate the effect of Anderson disorder for comparison with charge puddle situation. Fig.4 shows the Andreev reflection coefficient T_{11A} versus E under different Anderson disorder strength W with the superconductor phase difference $\theta = 0$ and π. In the case of a weak disorder strength (e.g.: $W = 50\Delta$), the shape of T_{11A} curves is found to be almost the same as the one in $W = 0$ situation in both cases $\theta = 0$ and $\theta = \pi$ (see Fig.4(a) and Fig.4(c)). Accordingly, the boundaries lying at $|E| = |E_0|$ are almost unchanged as well. With W

up to 200Δ and 400Δ, although the curves are slightly changed and the boundaries begin to weakly blur around $|E| = |E_0|$, it is still easy to clearly distinguish two kinds of Andreev reflections (see Fig.4(a) and (c)). Next we further increase the Anderson disorder strength to be comparable with the hopping energy t ($t = 2750\Delta$). In this situation Andreev reflections are affected much more greatly than smaller W, and the retroreflection and specular reflection become totally chaotic when W is around $3.0t$ (see Fig.4(b) and Fig.4(d)). In detail, T_{11A} decreases within the interval $[-|E_0|, |E_0|]$ and increases in the region $|E_0| < |E| < \Delta$ when $\theta = 0$, and the results reverse when $\theta = \pi$. However, we emphasize that while the disorder strength W reaches $0.5t$, two kinds of Andreev reflections can be still well distinguished, although the boundary is blurred a lot (see Fig.4(b) and Fig.4(d)).

By comparison between Fig.4 and Fig.2, we can see that the behaviors of the Andreev reflection coefficient under a larger Anderson disorder strength are similar to that under a rather weak electron-hole puddle disorder strength, and this can be explained as follows. In the tight-binding model, the hoping matrix element $t = \hbar^2/2m^*\tilde{a}^2$ is related to the lattice constant $\tilde{a}$.[36] For charge puddles model, the on-site energies of carbon atoms subject to Gaussian distribution. In real space, the on-site energies are correlated in short range and randomly distributed in long range. But for Anderson disorder model, the on-site energies of carbon atoms are randomly distributed both in short range and long range. Hence the correlation length of puddles is larger than that of Anderson disorder model. Therefore the influence of charge puddle model in the long range is similar to that of Anderson disorder model in the short range with a larger effective disorder strength. In Fig.3(c), for comparison the D-W relation is also shown for Anderson disorder case. Similar to the charge puddle situation, the net discrepancy value D increase monotonously with the increase of disorder strength W. However, now the value D/W is very small, e.g. for $W = 300\Delta$, D only is about 0.08 and $D/W \approx 0.0003$, indicating clearly that the Anderson disorder do have smaller effect than the charge puddles disorder.

Next we study the effect of disorders on Andreev reflections from another view, and investigate T_{11A} and T_{13A} as function of W at given incident electron energies E. The superconductor phase is set as $\theta = 0$, and the numerical results are shown in Fig.5. While without the disorders ($W = 0$), $T_{11A}(T_{13A})$ is exactly zero at $|E| > |E_0|$ and has finite values within $|E| < |E_0|$. With increasing disorder strength W, the values of T_{11A} (T_{13A}) decrease within $|E| < |E_0|$ but increase at $|E| > |E_0|$ for both charge puddles disorder and Anderson disorder, so that the boundary lying at $|E| = |E_0|$ becomes to blur. However, we can also see that, under a rather larger W (typical 30Δ as in experiment for charge puddles and 400Δ for Anderson disorder), the discrepancy between $T_{11A}(|E| < |E_0|)$ and $T_{11A}(|E| > |E_0|)$ is obvious, and so are the values of T_{13A}. This indicates that, in this situation the boundary at $|E| = |E_0|$ is just a little blurred so that two kinds of Andreev reflections can be clearly distinguished as well. Furthermore, from Fig.5 the behaviors of $T_{11A}(T_{13A})$ under charge puddles are similar to that under Anderson disorder, and only differ on the range of disorder strength. This result agrees with the above discussion as well as Fig.3.

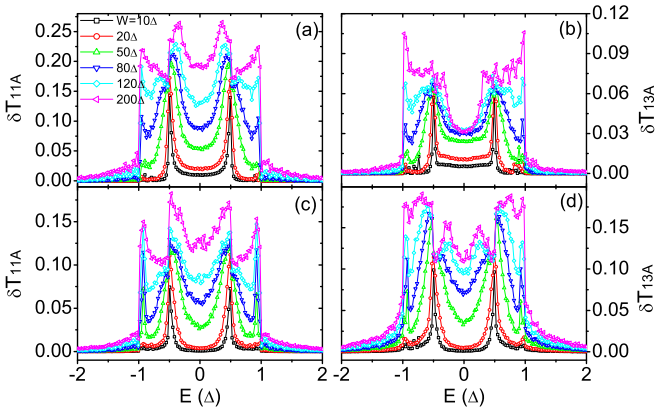

FIG. 6: (Color online) Fluctuations δT_{11A} and δT_{13A} versus energy E are shown under different charge puddle disorder strength W for $\theta = 0$ (in panel (a) and (b)) and $\theta = \pi$ (in panel (c) and (d)). The parameters unmentioned are the same as in Fig.2.

Let us study the fluctuation of T_{11A} and T_{13A} as function of energy E under different disorder strength W. The fluctuation of Andreev reflection coefficients is defined as $\delta T_{11(13)A} = \sqrt{\langle T^2_{11(13)A}\rangle - \langle T_{11(13)A}\rangle^2}$, in which $\langle T\rangle$ is the average of T over the disorder configurations. The numerical results for the charge puddles disorder are presented in Fig.6, from which it is clear to see that δT_{11A} and δT_{13A} have the peaks at $E = \pm|E_0|$ no matter $\theta = 0$ or $\theta = \pi$. Because that $E = \pm|E_0|$ is the boundaries of specular Andreev reflection and Andreev retroreflection and the Andreev reflection coefficients vary strongly when E passes $\pm|E_0|$. With increasing W, additional two peaks lying at $E = \pm|\Delta|$ emerge because that the Andreev reflection coefficients are large and have peaks at that E value. It demonstrates that the Andreev reflections are much more chaotic when the energy E is at around $|E_0|$ or Δ. Besides, under a typical disorder strength (e.g.: $W = 20\Delta$ or 50Δ), the fluctuations δT_{11A} (δT_{13A}) are found to be very small when energy E is away from the boundary $|E| = |E_0|$, again confirming that the boundaries of retroreflection and specular reflection well survive in the presence of charge puddles. In particular, due to that the fluctuation almost is zero while E is away from $\pm|E_0|$, the distinguishable feature of boundaries is not the consequence of averaging over a great deal disorder configurations. In other words, even if for an arbitrary specific disorder configuration, the boundaries of two Andreev reflections are still not blurred.

Finally let us discuss the case of the superconductor phase difference $\theta \neq 0$ or π. In this case, the Andreev

reflection coefficients have usually rather large values in whole region $[-\Delta, \Delta]$ even the impurity strength $W = 0$, because totally constructive or destructive interference can not be achieved at $\theta \neq 0$ and π. Now there is no clear boundary in the Andreev reflection coefficients. However, the two Andreev reflections still exist. It is the specular Andreev reflection while $|E| > |E_0|$ and the reflected hole is along the specular direction, otherwise at$|E| < |E_0|$ it is the Andreev retroreflection. So the two Andreev reflections still have a clear boundary at $|E| = |E_0|$. From above results, we can speculate that this boundary should maintain in the typical experimental impurity strength ($W = 20\Delta$). In fact, while $\theta \neq 0$ or π and $W < 30\Delta$, the fluctuation is still very small away from $\pm|E_0|$, which clearly indicates that the boundary blurring is small.

IV. CONCLUSIONS

In summary, by using a four-terminal graphene-superconductor hybrid system, we have studied how disorder in graphene affects the boundary of the specular Andreev reflection and Andreev retroreflection. Two kinds of disorders, the charge puddles and Anderson disorders, are considered. We find that the Andreev reflection coefficients are hardly affected while the charge puddle disorder strength has been much larger than superconductor gap (e.g. ten times), and the boundary at $|E| = |E_0|$ of the specular reflection and retroreflection can well maintain. Furthermore, even under very large disorder strength (e.g., one hundred times larger than the superconductor gap), two kinds of Andreev reflections can be still well separated and manipulated, and the boundary between them still clearly exists. We also study the effect of Anderson disorder for comparison, and found that the boundary at $|E| = |E_0|$ is held much more obviously in this case. In order to quantitatively describe to what degree the boundary is blurred, a quantity D is introduced, from which we confirm that the quantity D of the boundary blurring is much smaller than the disorder strength W, and D/W approximatively is 0.003 for the charge puddles disorder and 0.0003 for the Anderson disorder. The D-W relations for different values of the spatial correlation length η and the superconductor gap are studied as well. Finally, the fluctuations of Andreev reflection coefficient are studied. Under a typical experimental disorder strength (e.g. $W = 30\Delta$), the fluctuations are very small while energy E is away from the boundary $|E| = |E_0|$, again confirming that the retroreflection and specular reflection can be clearly distinguished and detected in the presence of disorder.

V. ACKNOWLEDGMENTS

This work was financially supported by NSF-China under Grants Nos. 10974236, 11004159, and 11074174, and the Natural Science Basic Research Plan in Shaanxi Province of China (No. 2010JQ1007).

* Electronic address: sunqf@iphy.ac.cn

[2] C. W. J. Beenakker, Rev. Mod. Phys. **80**, 1337 (2008).

[3] A. H. Castro Neto, F. Guinea, N. M. R. Peres, K. S. Novoselov and A. K. Geim, Rev. Mod. Phys. **81**, 109 (2009).

[4] A. K. Geim, Science **324**, 1530 (2009).

[5] N. M. R. Peres, Rev. Mod. Phys. **82**, 2673 (2010).

[6] K. S. Novoselov, A. K. Geim, S. V. Morozov, D. Jiang, Y. Zhang, S. V. Dubonov, I. V. Grigorieva, and A. A. Firsov, Science **306**, 666 (2004).

[7] K. S. Novoselov, A. K. Geim, S. V. Morozov, D. Jiang, M. I. Katsnelson, I. V. Grigorieva, S. V. Dubonos, and A. A. Firsov, Nature (London) **438**, 197 (2005).

[8] Y. Zhang, Y.-W. Tan, H. L. Stormer, and P. Kim, Nature (London) **438**, 201 (2005).

[9] T. Ando, J. Phys. Soc. Jpn. **74**, 777 (2005).

[10] M. I. Katsnelson, K. S. Novoselov, and A. K. Geim, Nature Phys. **2**, 620 (2006).

[11] V.V. Cheianov, V. Fal'ko, and B. L. Altshuler, Science **315**, 1252 (2007).

[12] J. R. Williams, L. Dicarlo, and C. M. Marcus, Science **317**, 638 (2007).

[13] W. Long, Q.-F. Sun, and J. Wang, Phys. Rev. Lett. **101**, 166806 (2008); J. Li and S.-Q. Shen, Phys. Rev. B **78**, 205308 (2008); S.-G. Cheng, J. Phys.: Condens. Matter **22**, 465301 (2010); J.-C. Chen, T. C. Au Yeung, and Q.-F. Sun, Phys. Rev. B **81**, 245417 (2010).

[14] H. Haugen, D. Huertas-Hernando, and Arne Brataas, Phys. Rev. B **77**, 115406 (2008); T. Yokoyama, Phys. Rev. B **77**, 073413 (2008).

[15] W. Tian and S. Datta, Phys. Rev. B **49**, 5097 (1994); S. Russo, J. B. Oostinga, D. Wehenkel, H. B. Heersche, S. S. Sobhani, L. M. K. Vandersypen, and A. F. Morpurgo, Phys. Rev. B **77**, 085413 (2008); P. Recher, J. Nilsson, G. Burkard, and B. Trauzettel, Phys. Rev. B **79**, 085407 (2009).

[16] M. Titov, and C. W. J. Beenakker, Phys. Rev. B **74**, 041401(R) (2006).

[17] S. Bhattacharjee and K. Sengupta, Phys. Rev. Lett. **97**, 217001 (2006); J. Cayssol, Phys. Rev. Lett. **100**, 147001 (2008).

[18] H. B. Heersche, P. Jarillo-Herrero, J. B. Oostinga, L. M. K. Vandersypen and A. F. Morpurgo, Nature (London) **446**, 56 (2007); F. Miao, S. Wijeratne, Y. Zhang, U. C. Coskun, W. Bao, C. N. Lau, Science **317**, 1530 (2007).

[19] C. W. J. Beenakker, Phys. Rev. Lett. **97**, 067007 (2006).

[20] A. F. Andreev, Sov. Phys. JETP. **19**, 1228 (1964).

[21] J. Linder, T. Yokoyama, D. Huertas-Hernando, and A. Sudbø, Phys. Rev. Lett. **100**, 187004 (2008); Q.Y. Zhang, D.Y. Fu, B.G. Wang, R. Zhang, D. Y. Xing, Phys. Rev. Lett. **101**, 047005 (2008); Q. Liang, Y. Yu, Q. Wang, and J. Dong, Phys. Rev. Lett. **101**, 187002 (2008).

[22] S.-g. Cheng, Y. X. Xing, J. Wang, and Q.-f. Sun, Phys. Rev. Lett. **103**, 167003 (2009).

[23] K. Nomura and A. H. MacDonald, Phys. Rev. Lett. **98**, 076602(2007); E. H. Hwang, S. Adam, and S. Das Sarma, Phys. Rev. Lett. **98**, 186806 (2007).
[24] M. S. Foster and I. L. Aleiner, Phys. Rev. B **77**, 195413 (2008).
[25] S. Cho and M. S. Fuhrer, Phys. Rev. B **77**, 081402(R) (2008).
[26] J. Martin, N. Akerman, G. Ulbricht, T. Lohmann, J. H. Smet, K. von Klitzing, and A. Yacoby, Nat. Phys. **4**, 144 (2008); Y.B. Zhang, V.W. Brar, C. Girit, A. Zettl and M.F. Crommie. Nature Physics **5**, 722 (2009).
[27] A. Deshpande, W. Bao, F. Miao, C. N. Lau, and B. J. LeRoy. Phys. Rev. B **79**, 205411 (2009).
[28] A. Deshpande, W. Bao, Z. Zhao, C. N. Lau, B. J. LeRoy, Appl. Phys. Lett. **95**, 243502 (2009).
[29] Th. Koschny and L. Schweitzer, Phys. Rev. B **67**, 195307 (2003); T. Kawarabayashi, Y. Ono, T. Ohtsuki, S. Kettemann, A. Struck, and B. Kramer, Physical Review B, **78**, 205303 (2008); T. Kawarabayashi, Y. Hatsugai, and H. Aoki, Phys. Rev. Lett. **103**, 156804 (2009).
[30] We first generate the correlated on-site energy $\tilde{\varepsilon}_j$ in a square lattice, and then map it into a honeycomb lattice. Because that the size of the puddles are much larger than the honeycomb lattice constant, thus the approximation is acceptable.
[31] Q.-f. Sun and X.C. Xie, J. Phys.: Condens. Matter **21**, 344204 (2009).
[32] D. H. Lee and J.D. Joannopoulos, Phys. Rev. B **23**, 4997 (1981); M. P. López Sancho, J. M. López Sancho and J. Rubio, J. Phys. F: Met. Phys. **14**, 1205 (1984); M. P. López Sancho, J. M. López Sancho and J. Rubio, J. Phys. F: Met. Phys. **15**, 851 (1985).
[33] Q.-F. Sun, J. Wang, and T.-h. Lin Phys. Rev. B **59**, 3831 (1999); **59**, 13126 (1999); Q.-f. Sun, B.-g. Wang, J. Wang, and T.-h. Lin, Phys. Rev. B **61**, 4754 (2000).
[34] G. E. Blonder, M. Tinkham, and T. M. Klapwijk, Phys. Rev. B **25**, 4515 (1982); G. Deutscher, Rev. Mod. Phys. **77**, 109 (2005).
[35] Q.-f. Sun and X. C. Xie, Phys. Rev. lett. **104**, 066805 (2010).
[36] *Electronic Transport in Mesoscopic Systems*, edited by S. Datta (Cambridge University Press 1995).